**Proceedings 2020 ASME International Manufacturing Science and Engineering Conference**
**MSEC2020**
**June 22-26, University of Cincinnati, USA**

# MSEC2020-8281

# ADVANCED SENSING DEVELOPMENT TO SUPPORT ACCURACY ASSESSMENT FOR INDUSTRIAL ROBOT SYSTEMS

**Guixiu Qiao**
National Institute of Standards and Technology
Gaithersburg, Maryland, USA

**Jonathan Garner**
University of Maryland
Collage Park, Maryland, USA

## KEY WORDS

Advanced Sensing, Condition Monitoring, Diagnostics, Prognostics Maintenance, Health Management, Industrial Robot Systems, Performance Degradation

## ABSTRACT

Manufacturers currently struggle with the assessment of a machine/robots' accuracy degradation that limits the efficiency of machine/robots in high precision applications. Current best practice in industry is to inspect the final products or add redundancies (local calibration, etc.) during the process to determine the machine's accuracy and performance. These create complexities in the process and increase the maintenance costs of applications such as high precision robot operations (welding, robotic drilling/riveting, and composite material layout), in-process metrology, and machines in mobile applications. A higher speed, more precise control of position and orientation is required to remedy these complexities. A novel smart target was designed at the National Institute of Standards and Technology (NIST) to integrate with a vision system to acquire high-accuracy, real-time 6-D (six-dimensional x, y, and z position, roll, pitch, and yaw orientation) information. This paper presents the development of the smart target and the image processing algorithm to output 6-D information. A use case is presented using the smart target on universal robots (UR3 and UR5) to demonstrate the feasibility of using the smart target to perform the robot accuracy assessment.

## INTRODUCTION

Machines and robots are key automation instruments that are widely used in manufacturing, material handling, construction, medicine, and aerospace [1]. In recent years, robots have become more accurate due to improvements in motion control, actuators, and other technologies [2]. These improvements enable the broader use of robots in many new applications. Machines and robots' accuracy assessment is crucial to these applications. Unexpected disturbances due to accuracy degradation may lead to a degradation of the system performance, causing losses in productivity and business opportunities [3]. With current industry practice, it is difficult to detect the accuracy degradation because the machine or robot is continuously running and appears to be making parts that wouldn't not meet the quality requirements, including accuracy requirement.

As shown in Fig. 1, the typical robot errors contain static errors and dynamic errors. Static errors of a 6-axis robot include geometric error (e.g., linkage length, tools, and object in workspace), elasticities (e.g., base, runout, and gears), and temperature change created errors (quasi-static errors); dynamic errors include the trajectory following errors, gear cyclic errors, and axis dynamic limits [2, 4]. Because these errors influence robots' absolute accuracy, traditional hard automation must depend on robot teaching, which is very time-consuming thus increasing the costs of manufacturing. To work around the accuracy problems, many extra sensors and redundancies are added. For example, flexible grippers or extra sensors are implemented to increase task tolerance. Local calibrations are developed to improve local accuracy for the success of precision operations. Sometimes external guidance, for example, a laser tracking system, is added to guide the robot's precision operations [5, 6]. These workaround methods significantly increase the complexity of the manufacturing system and the cost of system maintenance. Moreover, there are new emerging robot applications that require more precise robot operations, for example, high precision assembly, welding, robotic drilling/riveting, robot metrology, and composite material layout. There needs to be an innovative way to design new robot systems instead of continuously using 20-year-old methods. The robot accuracy needs to be measured, assessed, monitored, and improved to support the development of an optimized and simplified production line by enhancing the absolute accuracy. Moreover, economic factors also motivate facilities and factories to perform accuracy degradation assessment and monitoring the robot performance to detect faults and failures. The purpose is to improve maintenance techniques and operations, especially eliminating unexpected shutdowns.

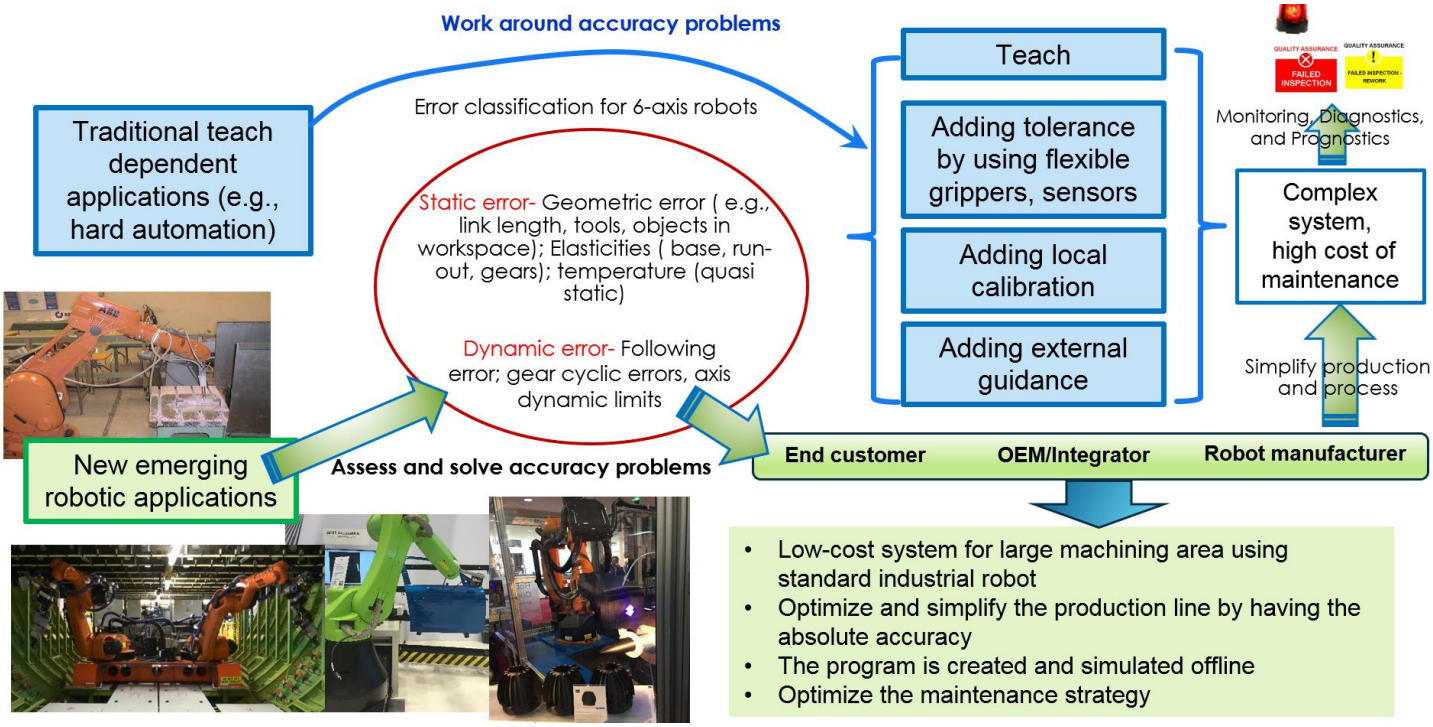


Figure 1. Robot accuracy degradation and influences

A robot's position (x, y, z) and orientation (pitch, yaw, roll) need to be measured to assess the robot's accuracy. The measured 6-D information can be used to calculate the deviations of robot position and orientation, allowing for accuracy degradation monitoring of a robot. The data can also be used as feedback for more accurate control, or as the input of an algorithm to perform calibration for robot performance improvement.

A novel smart target (patent pending) was developed at the National Institute of Standards and Technology (NIST) to integrate with a vision system to acquire high accuracy 6-D information of a moving object. The smart target is mounted on the object of interest, for example, the end effector/tool of a robot arm or the last link of a machine tool to measure/track the object's 6-D position and orientation. The smart target development is a part of the Prognostics and Health Management for reliable operations in Smart Manufacturing (PHM4SM) research at NIST. The PHM4SM project works on developing and deploying measurement science to promote the implementation, verification, and validation of advanced monitoring, diagnostic, and prognostic technologies to increase reliability and decrease downtime in smart manufacturing systems. This paper will present the research background, advanced sensing development, and a software tool to efficiently measure, monitor, diagnose, predict, and maintain the health of a robot. A use case was developed at NIST using Universal Robot UR3 and UR5 to demonstrate the feasibility of the smart target in accuracy assessment application.

## RESEARCH BACKGROUND AND APPROACH

There are various measurement systems to acquire 3-D/6-D information [7, 8]. Some old methods including gauges, pose matching, and coordinate measurement machines are very slow. Trilateration with a theodolite, using cable potentiometer systems, or laser interferometers and other methods usually lack orientation information [9-13]. The laser tracker and vision-based system are gaining more attention in recent years.

Laser trackers are one type of high precision 3-D/6-D measurement system [18]. As an important part of the measurement system, measurement targets define what dimensional information can be captured by the system. If a 3-D target is used, 3-D information is captured. If a 6-D target is used, 6-D information is captured. Retro-reflective spheres are an example of a 3-D target for laser trackers. A laser tracker tracks the target to measure distance from the reflected laser beam. Encoders on the laser tracker provide two angular orientations of the tracker's two mechanical axes. By combining the distance and two encoders' angles, the center (x, y, z) of the retro-reflective target is measured [14, 16]. For 6-D information measurement, extra sensors are added to the existing 3-D target, for example, multiple light-emitting diodes (LEDs), thus making a already-expensive system more complex. The retro-reflective target needs to be held in contact with the object of interest. Also, laser tracker systems need to maintain line-of-sight between the laser tracker and the target. This means that the tracker will ultimately lose its view of the target when observing the target on a robot rotating to an angle.

Vision-based systems have the advantages of cost-effectiveness and broader application potentials with advanced image processing technology. The vision-based system includes camera array and structured light technology.

The camera array approach uses multiple cameras placed at different positions to capture multiple images of the same target [17, 19]. A dual-camera system is the simplest yet most popular camera array. Two cameras are separated by a distance, usually with a similar angle of view to benefit the disparity calculation. For each point in space, there is a measurable disparity between its positions in the two camera images. The depth of the point is then calculated using geometry. The main challenge of a camera array is how to find matching points in multiple images with good accuracy. Non-ideal point matching decreases the system's accuracy. Particularly, when multiple cameras are placed with a certain angle to enlarge the overlap of cameras' imaging for larger measurement capability, the non-ideal point matching problem gets more severe. Also, when the measured parts do not have enough features, for example, a smooth surface, the measurement accuracy decreases.

Structured light is an example of a special version of a camera array. Additional active projectors are added to solve the image matching problem in camera array. Projected patterns include fringes, random pattern laser dots, or other known patterns. These known patterns created a phase map to match the matching points in multiple images. A receiver detects the distortion of the reflected pattern to calculate a depth map based on geometry. The structured light system has better depth accuracy performance compared to the camera array system. However, the structured light system may be more expensive because of the costs of active projectors.

Both the camera array and structured light system are sensitive to environmental light. For the camera array, a bright environment works best. Structured light systems work best in a dark environment. When the brightness of the environment changes, images captured by a camera array may become noisy, and contrast becomes poor. This makes point matching extremely difficult resulting in inaccurate depth estimates. Moreover, structured light systems usually need to scan through a set of projected patterns. The measurement instrument and the measured part need to stay stationary during the measurement, which is not suitable for dynamic measurement.

Thus, although a variety of 6-D measurement systems and targets are available, these conventional systems do not have acceptable accuracy and dynamic features that are sufficiently accurate as required by some applications. As such, a new smart target was developed at NIST working with vision-based systems to overcome the challenges presented by complex industrial environments, enabling the measurement of dynamic poses.

## ADVANCED SENSING DEVELOPMENT

The smart target system (patent pending) is a novel design to exceed the performance of existing vision-based measurement systems, especially with respect to accuracy and real-time processing potential. As shown in Fig. 2, the smart target consists

Figure 2. NIST designed smart target

of fixed-wavelength light pipes and two high-precision rotary gimbals. Three cylindrical light pipes, each a different color, are used to define line features that construct the 6-D information of a coordinate frame. The fixed-wavelength design makes the target stand out from an industrial background. At the same time, the target is not sensitive to environmental light. The red cross allows the vision system to detect the cross center as a coordinate origin. The gimbals are motorized to constantly rotate the red cross toward the measurement instrument for non-blocking dynamic measurement. It maximizes the target's line-of-sight to the vision system, thereby reducing measurement uncertainty. The blue and green pipes move with the object of interest and allow the camera system to determine orientation. This novel design enhances the matching of features across multiple images, especially in the presence of complex, industrial backgrounds. The smart target is mounted on the object of interest, for example, the end effector or tool of a robot arm, or the last link of a machine tool to measure and track the object's 6-D position and orientation. The smart target provides:

1) High accuracy. Traditional targets have large uncertainty in measuring orientation. The most common traditional targets for vision systems are spheres. With infrared camera systems, the spheres are coated with reflective material or wrapped with reflective tapes. The center of the sphere is the feature to be measured. Multiple spheres are put together to define a coordinate frame. One sphere center may be used to define the origin of the coordinate frame. An axis is defined by two spheres centers. For this type of target, the measurement uncertainties of the sphere center are transferred one-to-one to the coordinate origin definition. Since only two points are used to define the axial direction, the angle measurement uncertainties are enlarged since a small distance error of the sphere center can create a large angular error. On the contrary, the axial direction of the smart target is defined using many points along the cylindrical target's centerline. Thus, the constructed center line is more accurate by fitting multiple points instead of only two points. For the same reason, the origin of the coordinate is created by intersecting two centerlines, which leads to an accuracy increase of 3 times compared to the traditional method of defining the origin using a sphere center. Moreover, extra features of the light pipe, including the fixed-wavelength color, the edge features of cylinders, etc., give more redundant information to improve the line detection accuracy.

2) Non-blocking measurement design to measure both static and dynamic robot tool center point (TCP) data. Traditional targets have the problem of bad pose (perpendicular to the

camera) when the target pose is not sensitive to camera measurement, or the target may block itself in some poses. The smart target has the red cross mounted on rotary axes. The red cross can constantly rotate toward the measurement system. The red cross center is defined as the coordinate system's origin. The rotation mechanism makes the smart target's origin good for measurement in different views without self-blocking.

3) A unique definition of a coordinate frame. Traditional spherical targets do not have a unique definition of a frame. With the bad pose problem, spheres that define the origin may be blocked for measurement. Traditional sphere targets usually use best-fit transformation to find translation and rotation of two sets of center points. Best-fit usually uses the minimum least square errors for the conversing condition, thus not guaranteeing the consistent and minimum error for the origin. The 6-D smart target has a consistent and unique definition of a frame to avoid confusion when multiple coordinates exist in a system.

The 6-D smart target allows the continuous measurement of the 6-D information of a moving object with high accuracy. Applications of the smart target can be any general measurement system that requires high accuracy 6-D information of a moving object, for example, the robot and machine calibration, or multiple machines/tools/objects registrations, or adaptive objects location for unplanned adaptive control, or precisely tracking the pose of an object.

## SOFTWARE TOOL DEVELOPMENT

A software tool is needed to process smart target-captured images, extract features, and output 6-D data. Software development was divided between creating a graphical user interface (GUI) to interface with the stereo camera system and designing and implementing an image processing algorithm to identify the smart target and determine its position using stereo images.

The GUI interfaces with the stereo camera system to allow for image processing is shown in Fig. 3. The software implements basic features such as image capture from each camera, video recording from one or both cameras, video playback, live video feeds, and smart target identification. An event handler responds to cameras connecting and disconnecting, as well as image transfer including transfer errors. The software receives images from the two cameras, displays them, and processes them as the user desires.

Figure 3. GUI to interface with the stereo camera system

While the GUI is receiving images from the cameras, the smart target can be tracked. An area of interest is drawn around the smart target in the live video feeds on the GUI to indicate the portion of the image to be used for further processing for location and orientation.

The image processing algorithm uses multiple layers of processing to identify the smart target and extract its location in 3D space. A software filter is applied to images from the two cameras to accentuate the red, blue, and green colors of the smart target. The filter accentuates both the horizontal and vertical cylinders of the red cross so the two can be distinguished. In each image, an area of interest (AOI) is found that encompasses the entire target as shown in Fig. 4 (a). The AOI reduces the size of the frame that must be further processed to reduce processing time for each frame.

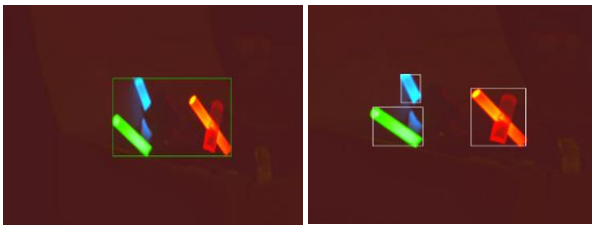

(a) (b)

Figure 4. Identify target from complex background

To find the AOI, a threshold filter is applied to identify the bright smart target. A morphological opening is also applied to reduce noise and to remove unwanted pixels that pass through the threshold filter. The detected AOI is drawn on top of live video feed on the GUI to display the part of the frame that will be processed further. To identify the three parts of the smart target and differentiate them based on color, a HSV filter is used. The three parts of the smart target can be identified (as shown in Fig. 4 (b)).

The next important part of the image processing is to identify the center lines of the green and blue cylinders and the center point of the red cross. The center of the red cross is found by finding the intersection of the lines running through the center of the red cross. A Laplacian of Gaussian (LOG) filter is applied to each colored part of the smart target. The filter marks the edges of the cylinder by a sharp jump from negative intensity to positive intensity. The zero crossing on each edge can be found and from there the centerline. Zero crossings on either side of the cylinder correspond with a point along the center of the cylinder. A line of best fit is found through the center points (Fig. 5 (a)). The center points, shown in black in Fig. 5 (a), come from the

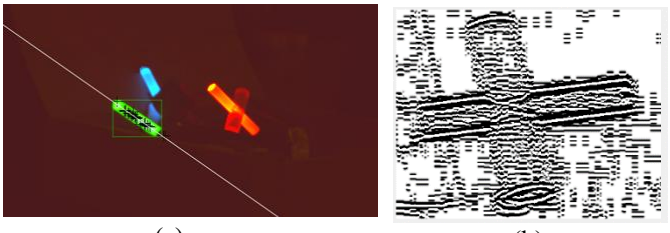

(a) (b)

Figure 5. Feature detection of the smart target

edges of the cylinder. The line of best fit, shown in white in Fig. 5 (a), is found from the center points.

The red cross presents a challenge due to its more complex shape and unequal lighting. One cylinder of the red cross is evenly lit while the other is dim and uneven. This requires different processing techniques for the two parts. The evenly lit section of the cross is processed the same way as the blue and green cylinders using a LOG filter. The output of the Laplacian of Gaussian filter is shown in Fig 5 (b). The bright cylinder of the cross is the horizontal cylinder in Fig. 5 (b), and the dark cylinder is the vertical cylinder.

After the LOG filter, the two edges of the cylinder are found, then the center points, and the line of best fit of the centerline. The darker cylinder of the red cross is processed using a Canny filter to clearly identify the weaker edges of the vertical cylinder as shown in Fig. 6 (a). The Canny filter is not used in place of the LOG filter in other parts of the processing as it is prone to noise and weak edges found in the background. The LOG filter is more effective at singling out the edges of the bright cylinders. The results of the two processing methods for the cross are combined to find the center point of the red cross (Fig. 6 (b)). To determine the smart target position in 3D space, the location of the red cross center point, and the line of best through the green and blue cylinders are used from the two stereo images. The image pixel coordinates of the red cross and equations of the two lines are undistorted and normalized to using parameters from the camera calibration to account for distortion in the camera lenses. Camera calibration is determined beforehand and loaded into the GUI for processing. The camera calibration includes information such as focal length, rotation matrix, and translation vector between the two stereo cameras.

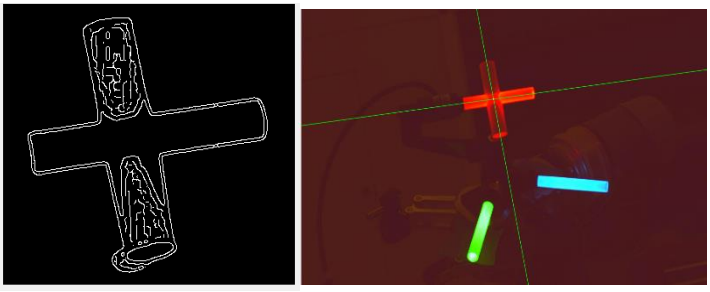

(a) (b)

Figure 6. Center point identification on red cross

The 2-D to 3-D construction uses two cameras calibrated poses (not detailed in this paper). In each camera, a vector is found from the pinhole camera origin to the cross center. The intersection of the two vectors is found as the location of the red cross in 3D space as shown in Fig. 7.

For both green and blue cylinders from the two images, a plane is found using the origin and the specific line. The line of intersection of the corresponding blue or green planes between the two frames is found. This line of intersection is the centerline through the green or blue cylinder in 3D space.

The position information about the smart target can be displayed on the GUI and will update with each new pair of

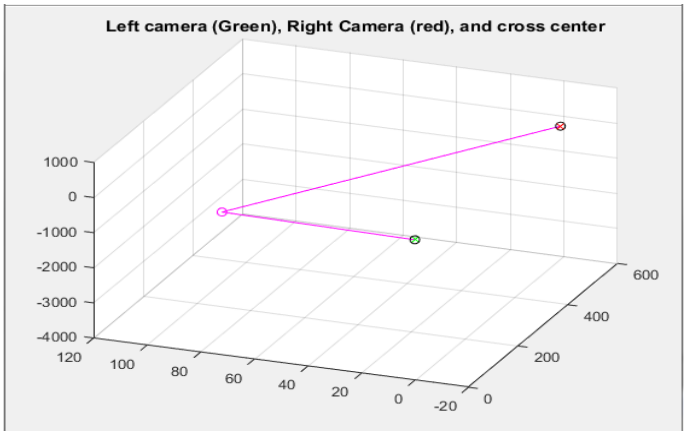


Figure 7. Intersecting vectors from pinhole cameras to center of the red cross

images from the cameras. The position data is also written to a user-specified file with a timestamp. The next step is to optimize the algorithm to speed up the calculation. To capture dynamic movement, the measurement speed needs to be above 30 frames per second. Adding GPU (Graphics Processing Unit) and parallel calculation will help to speed up the image processing process.

## USE CASE DEVELOPMENT

NIST is developing a quick health assessment methodology using a smart target to assess the accuracy degradation of the TCP throughout the robot workspace. The methodology includes the advanced sensing development (the smart target) to acquire the robot TCP's 6-D information, a test method to define the robot movements and a robot error model to reflect the robot geometric and non-geometric errors, and algorithms to process measured data to assess the robot's accuracy degradation.

As shown in Fig. 8 (a), the 6-D smart target is mounted on the last joint of the UR3 robot. A vision-based measurement instrument is set up in the environment, which is at the opposite end of the kinematic chain from the target. The idea is to compare the measured TCP position to nominal positions. A set of predefined robot movements is created (as shown in Fig. 9) based upon the robot's kinematics, geometry, available working volume, and expected operational activities. The left picture of Fig. 9 shows the generation of the target positions. The right picture of Fig. 9 shows the simulation of the robot moving to the

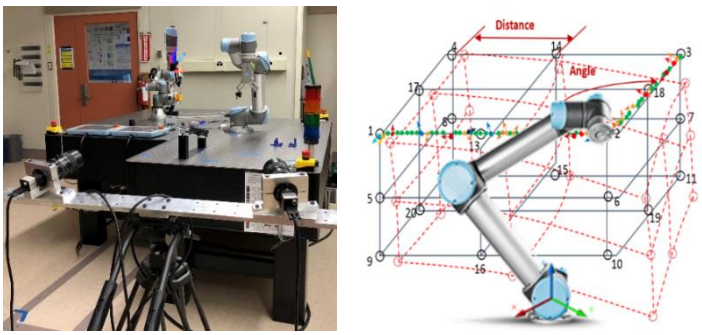


Figure 8. Use case setup for robot quick health assessment

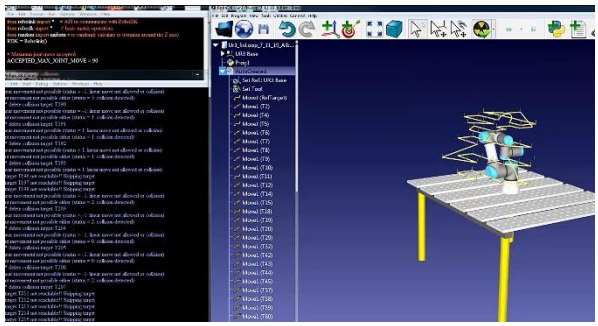

Figure 9. Auto-generation of pre-defined robot movement for quick health assessment

planned positions with collision detection algorithms embedded. Unreachable positions or positions having collision problem is removed and updated in the display. The robot movement is measured by the vision-based instrument. The measured TCP 6-D data is used to calculate the deviations from robot normal positions. The calculated deviations are input into the robot error model. The error model handles both the geometric/non-geometric errors and the uncertainties of the measurement system. An algorithm is developed to process the data to assess the robot's accuracy degradation [15]. The first output is the derived error from the calculation of the robot tool center accuracy of the robot through the workspace Fig. 8 (b). The results are more accurate because they are derived from the error model instead of directly calculating from the limited size of sample measurements. This output can be used to view the overall accuracy of a robot within the working volume and find the sweet zone of the robot where the accuracy is suitable for production. The second output is the identified maximum likelihood estimation of axis error parameters. By observing the error pattern, users can monitor the change of robot accuracy. Further analysis can be used to identify the potential error sources of the given errors (for example, zero shift of a joint encoder).

The quick health assessment can be used to swiftly (within 10 minutes) detect degradations in robot accuracy by finding the robot pose deviations from the nominal poses. The use of this methodology will monitor the degradation of robot performance, reduce unexpected shutdowns, and help the optimization of maintenance strategy to improve productivity.

## CONCLUSION

Accuracy degradation impacts machine/robot's performance. NIST's development of smart target can be integrated with a vision system to acquire high accuracy position and orientation information of a moving object, allowing for machine/robot's accuracy degradation assessment and accuracy improvement. This paper presented the novel design of the smart target and a software tool. With smart target's measurement, deviations of machine/robot position and orientation are quantified, leading to more accurate calibration or control, improving overall performance. NIST is seeking to develop additional industrial use cases for further applications.

## NIST DISCLAIMER

Certain commercial entities, equipment, or materials may be identified in this document in order to illustrate a point or concept. Such identification is not intended to imply recommendation or endorsement by NIST, nor is it intended to imply that the entities, materials, or equipment are necessarily the best available for the purpose.

## REFERENCES


[1] A. D. Pham and H. J. Ahn, "High precision reducers for industrial robots driving 4th industrial revolution: state of arts, analysis, design, performance evaluation and perspective," International Journal of Precision Engineering and Manufacturing-Green Technology, vol. 5, pp. 519-533, Aug 2018.

[2] A. Buschhaus, A. Blank, C. Ziegler, and J. Franke, "Highly Efficient Control System Enabling Robot Accuracy Improvement," Procedia CIRP, vol. 23, pp. 200-205, 2014.

[3] A. Cachada, J. Barbosa, P. Leitño, C. A. S. Gcraldcs, et al., "Maintenance 4.0: Intelligent and Predictive Maintenance System Architecture," in 2018 IEEE 23rd International Conference on Emerging Technologies and Factory Automation (ETFA), 2018, pp. 139-146.

[4] D. D. Chen, P. J. Yuan, T. M. Wang, Y. Cai, and L. Xue, "A Compensation Method for Enhancing Aviation Drilling Robot Accuracy Based on Co-Kriging," International Journal of Precision Engineering and Manufacturing, vol. 19, pp. 1133-1142, Aug 2018.

[5] J. Kim, A. Kawamura, Y. Nishioka, and S. Kawamura, "Mechanical design and control of inflatable robotic arms for high positioning accuracy," Advanced Robotics, vol. 32, pp. 89-104, 2018.

[6] D. Culla, J. Gorrotxategi, M. Rodriguez, J. B. Izard, P. E. Herve, and J. Canada, "Full Production Plant Automation in Industry Using Cable Robotics with High Load Capacities and Position Accuracy," in Robot 2017: Third Iberian Robotics Conference, Vol 2. vol. 694, A. Ollero, A. Sanfeliu, L. Montano, N. Lau, and C. Cardeira, Eds., ed Cham: Springer International Publishing Ag, 2018, pp. 3-14.

[7] Q. Guixiu, "Advanced Sensor and Target Development to Support Robot Accuracy Degradation Assessment," in 2019 IEEE 15th International Conference on Automation Science and Engineering (CASE), 22-26 Aug. 2019, Piscataway, NJ, USA, 2019, pp. 54-9.

[8] N. Zaimovic-Uzunovic and S. Lemes, "Cylindricity Measurement on a Coordinate Measuring Machine," in Advances in Manufacturing, A. Hamrol, O. Ciszak, S. Legutko, and M. Jurczyk, Eds., ed Cham: Springer International Publishing Ag, 2018, pp. 825-835.

[9] T. F. Shu, S. Gharaaty, W. F. Xie, A. Joubair, and I. A. Bonev, "Dynamic Path Tracking of Industrial Robots

With High Accuracy Using Photogrammetry Sensor," ASME Transactions on Mechatronics, vol. 23, pp. 1159-1170, Jun 2018.

[10] N. Y. Shen, Z. M. Guo, J. Li, L. Tong, and K. Zhu, "A practical method of improving hole position accuracy in the robotic drilling process," International Journal of Advanced Manufacturing Technology, vol. 96, pp. 2973-2987, May 2018.

[11] R. Schares, S. Schmitt, M. Emonts, K. Fischer, R. Moser, and B. Fruhauf, "Improving Accuracy of Robot-Guided 3d Laser Surface Processing by Workpiece Measurement in a Blink," in High-Power Laser Materials Processing: Applications, Diagnostics, and Systems Vii. vol. 10525, S. Kaierle and S. W. Heinemann, Eds., ed Bellingham: SPIE-Int Soc Optical Engineering, 2018.

[12] E. Pivarciova, P. Bozek, Y. Turygin, I. Zajacko, A. Shchenyatsky, S. Vaclav, et al., "Analysis of control and correction options of mobile robot trajectory by an inertial navigation system," International Journal of Advanced Robotic Systems, vol. 15, p. 15, Jan 2018.

[13] H. Gattringer, M. Neubauer, D. Kaserer, and A. Muller, "A Novel Method for Geometric Robot Calibration Using Laser Pointer and Cameras," in Advances in Service and Industrial Robotics. vol. 49, C. Ferraresi and G. Quaglia, Eds., ed Cham: Springer International Publishing Ag, 2018, pp. 200-207.

[14] R. Mautz, "Overview of current indoor positioning systems," Geodesy and Cartography, vol. 35, pp. 18-22, 2009.

[15] G. Qiao and B. A. Weiss, "Industrial Robot Accuracy Degradation Monitoring and Quick Health Assessment," Journal of Manufacturing Science and Engineering, Transactions of the ASME, vol. 141, 2019.

[16] R. Ahmad and P. Plapper, "Safe and Automated Assembly Process using Vision Assisted Robot Manipulator," Procedia CIRP, vol. 41, pp. 771-776, 2016.

[17] A. Filion, A. Joubair, A. S. Tahan, and I. A. Bonev, "Robot calibration using a portable photogrammetry system," Robotics and Computer-Integrated Manufacturing, vol. 49, pp. 77-87, Feb 2018.

[18] Y. B. HuangFu, L. B. Hang, W. S. Cheng, L. Yu, C. W. Shen, J. Wang, et al., "Research on Robot Calibration Based on Laser Tracker," in Mechanism and Machine Science. vol. 408, X. Zhang, N. Wang, and Y. Huang, Eds., ed Singapore: Springer-Verlag Singapore Pte Ltd, 2017, pp. 1475-1488.

[19] M. Ulrich, A. Forstner, and G. Reinhart, "High-accuracy 3D image stitching for robot-based inspection systems," in 2015 IEEE International Conference on Image Processing, ed New York: IEEE, 2015, pp. 1011-1015.